Supporting Information

A Copper(Ⅰ)-Catalyzed Azide-Alkyne Click Chemistry Approach towards Multifunctional Two-Way Shape-Memory Actuators

Zhong-Cheng Liu, Bo Zuo, Hai-Feng Lu, Meng Wang, Shuai Huang, Xu-Man Chen, Bao-Ping Lin, Hong Yang*

School of Chemistry and Chemical Engineering, Jiangsu Province Hi-Tech Key Laboratory for Bio-medical Research, Jiangsu Key Laboratory for Science and Application of Molecular Ferroelectrics, Institute of Advanced Materials, Southeast University, Nanjing, 211189, China

*Correspondence and requests for materials should be addressed to H.Y. (email: yangh@seu.edu.cn).

Materials

Copper(I) bromide (CuBr), 4-hydroxybenzoic acid and hydroquinone were purchased from Aladdin Inc. 10-Chloro-1-decanol was used as received from Alligator Reagent Inc. 11-Dodecyn-1-ol was purchased from Shanghai Udchem Technology Co. Ltd. Sodium azide was purchased from Great Wall Reagent Inc. Pentaerythritol was purchased from Shanghai Yuanye Biological Technology Co. Ltd. 6-Heptynoic acid was purchased from Bidepharmtech Co. Ltd. L-Proline, p-toluenesulfonic acid (TsOH) monohydrate, copper(I) iodide, tetrahydrofuran (THF), triphenylphosphine (PPh$_3$), N,N,N',N'',N''-pentamethyldiethylenetriamine (PMDETA) and diethyl azodicarboxylate (DEAD) were purchased from Energy Chemical Inc. Dimethyl sulfoxide, sodium hydroxide, sodium carbonate and ethyl acetate were purchased from Sinopharm Chemical Reagent Co. Ltd.

Methods

All ^{1}H NMR spectra and ^{13}C NMR spectra were obtained from a Bruker HW600 MHz spectrometer (AVANCE AV-600) using DMSO-d$_6$ (δ 2.50 ppm) or CDCl$_3$ (δ 7.26 ppm) as the solvent. Differential scanning calorimetry (DSC) spectra were recorded on a TA Instruments Q200 instrument (New Castle, DE) under nitrogen purge at both heating and cooling rates of 20 °C/min.

Polarized optical microscopy (POM) equipped with an Olympus BX53P microscope and a Mettler PF82HT hot stage were used to observe the mesomorphic properties of monomers and LCE films. The images were captured using a Microvision MV-DC200 digital camera with a Phenix Phmias 2008 Cs Ver2.2 software.

All mechanical property measurements of the MCLCEs were performed on adynamic mechanical analyzer (DMA Q800, TA Instrument) using tension clamp. The examined actuator ribbons were prepared with a dimension of ca. 3.0 cm long ×0.5 cm wide × 0.03 cm thick. In the elastic modulus experiments, the MCLCE samples were fixed on the instrument using the controlled force mode, and the set

temperatures were 30 °C, 60 °C, 90 °C, 110 °C, 120 °C, 130 °C and 140 °C respectively. After reaching the set temperature, the sample was kept at the constant temperature for 5 min, and then the stress-strain curves were measured when the tensile force rose to 18.00 N at a rate of 0.10 N/min. In the two-way shape memory effect (2W-SME) experiments, the MCLCE sample was fixed on the instrument using the isoforce mode, and the sample was heated and cooled for six cycles between 15 °C and 145 °C under a preload force of 0.001 N at a rate of 5.00 °C/min to give a thermal-induced shape memory curve. In the actuation stress (contractile force) experiments, the MCLCE sample was fixed on the instrument using the isostrain mode, the generated contractile force by the sample was measured along with the temperature variation when the sample was elongated by a fixed 0.01% strain in tension.

Thermogravimetric analysis (TGA) was measured by a Perkin-Elmer TGA7 under nitrogen atmosphere. Differential scanning calorimetry (DSC) spectra were obtained on a TA Q200 instrument under nitrogen atmosphere at both heating and cooling rates of 20 °C/min. One-dimensional and two-dimensional small-angle X-ray scattering (SAXS) patterns were recorded on a high-flux small angle X-ray scattering instrument (SAXSess, Anton Paar) equipped with a Kratky block-collimation system and a temperature control unit (Anton Paar TCS300).
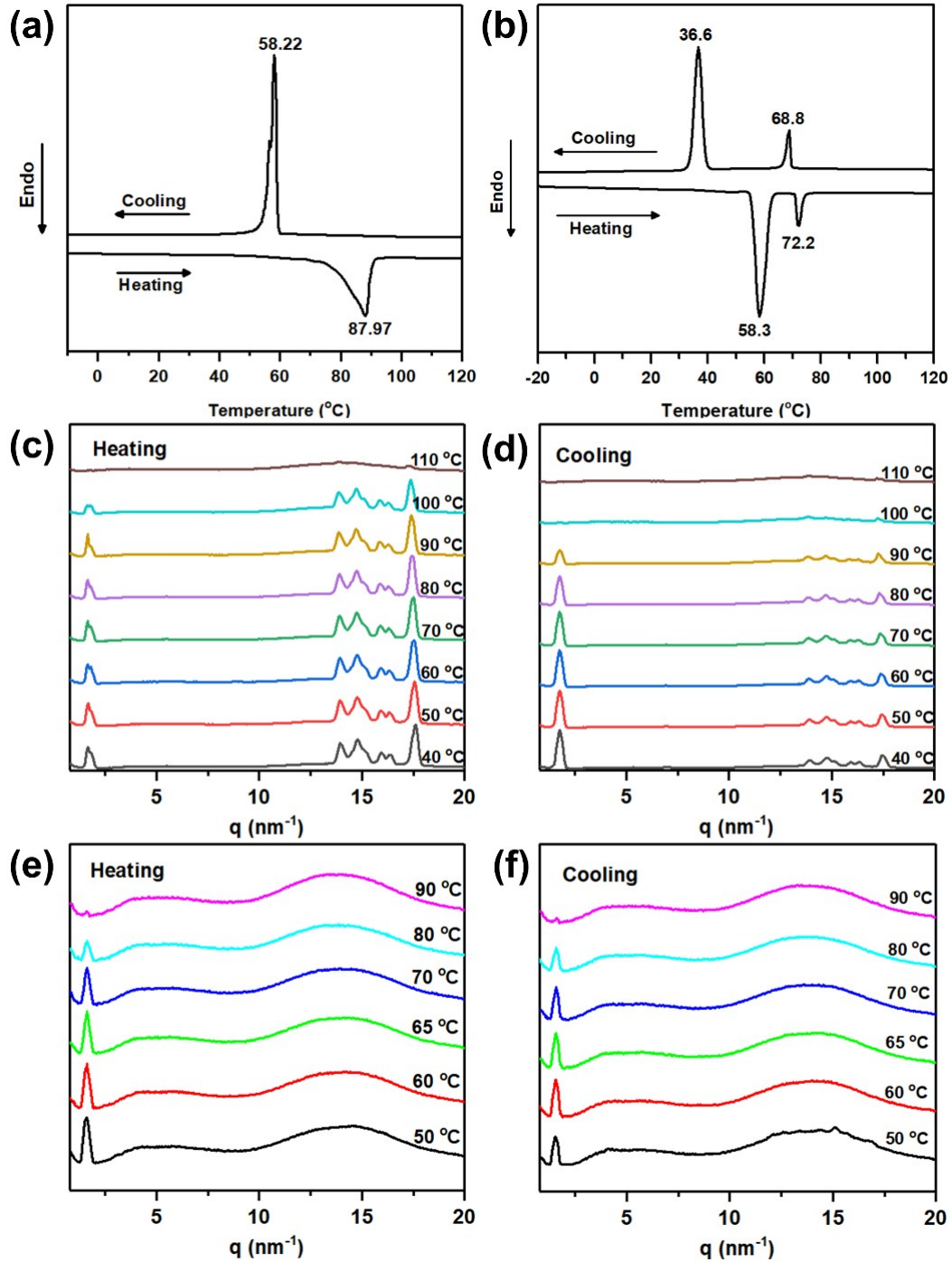
Fig. S1 DSC curves of (a) DPDB during the first cooling cycle and the second heating cycle at a rate of 20 °C/min under N_2 and (b) APAB during the first cooling cycle and the second heating cycle at a rate of 10 °C/min under N_2. One-dimensional SAXS patterns of DPDB during (c) the heating cycle and (d) the cooling cycle. One-dimensional SAXS patterns of APAB during (e) the heating cycle and (f) the cooling cycle.
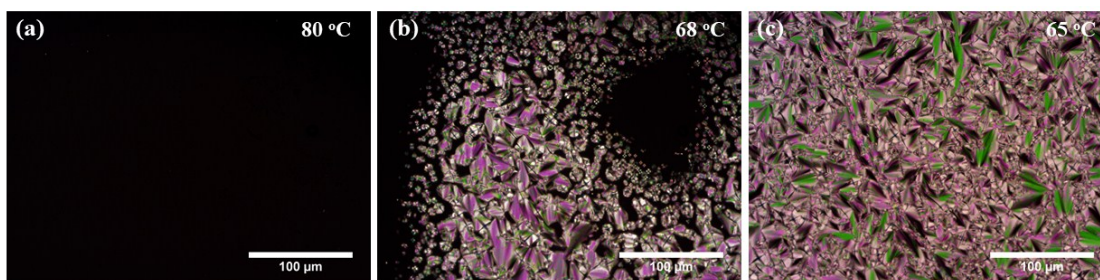
Fig. S2 POM images of monomer APAB recorded at (a) 80 $^{\circ}$C, (b) 68 $^{\circ}$C and (c) 65 $^{\circ}$C during the cooling process.

As shown in **Figure S1**a, during the first cooling and the second heating cycles, there was only one phase transition existed in monomer DPDB. Moreover, there were some obvious crystal diffraction peaks in the wide-angle region of **Figure S1**c,d. According to DSC and SAXS data, the monomer DPDB had no LC phase.

As shown in **Figure S1**b, monomer APAB exhibited two phase transitions during both the first cooling and the second heating cycles (on heating: Crystal – 58.3 $^{\circ}$C – LC – 72.2 $^{\circ}$C – Isotropic, on cooling: Isotropic – 68.8 $^{\circ}$C – LC – 36.6 $^{\circ}$C – Crystal). In addition, as shown in **Figure S2**, focal-conic texture was clearly observed in the APAB sample at 68 $^{\circ}$C during the cooling process.

As demonstrated in Figure S1e,f, one diffraction peak appeared at 4.08 nm in small-angle region during the heating and cooling processes, which was in agree with the fully extended length (l = 4.02 nm) of APAB, as estimated by Dreiding models. It could be inferred that APAB was assigned to smectic A phase (on heating: Crystal – 57.9 $^{\circ}$C – SmA – 71.9 $^{\circ}$C – Isotropic, on cooling: Isotropic – 69.8 $^{\circ}$C – SmA – 32.7 $^{\circ}$C – Crystal), based on the combination of POM images and SAXS results.
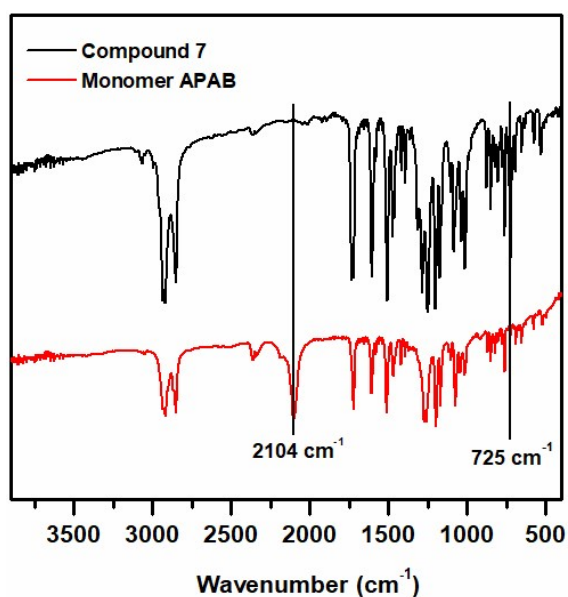
Fig. S3 FT-IR spectra of compound **7** and APAB.

As illustrated in **Figure S3**, FT-IR spectra of compound **7** and monomer APAB were examined . Apparently, monomer APAB showed a sharp absorption peak at 2104 cm^{-1} while compound **7** did not have this peak, and this peak was assigned to the azide group. Based on the results of ^{1}H NMR, ^{13}C NMR and IR spectra, it was concluded that APAB has been successfully synthesized from a substitution reaction between sodium azide and compound **7**.
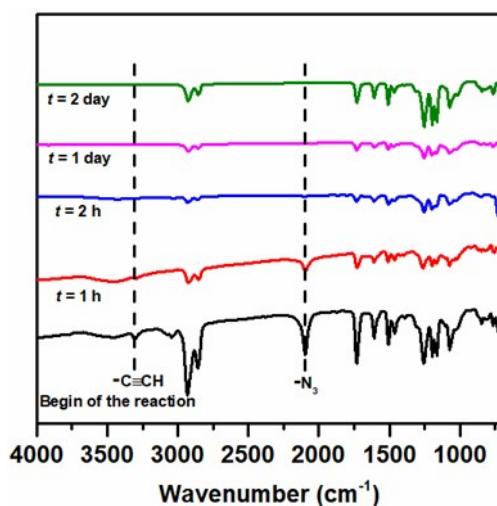
Fig. S4 FT-IR spectra of the azide-alkyne reaction mixture measured at 0 h, 1 h, 2 h, 24 h and 48h respectively.

In addition, we measured the FT-IR spectra of the reaction mixture at 0 h, 1 h, 2 h and 2 d. As shown in **Figure S4**, after pre-crosslinked at 55 °C for 2 h, there were still some unreacted azide and alkyne units in the polydomain MCLCE sample. Furthermore, the purpose of the second cross-linking of the polydomain MCLCE sample at 80 °C for two days was not only to complete the CuAAC reaction, but also to fix the orientational order of the mesogenic film to prepare the desired monodomain MCLCE material.

As shown in **Figure S5**, the C≡CH (3200~3400 cm^{-1}) belonging to monomer DPDB and the azide group signals (2100~2300 cm^{-1}) belonging to monomer APDB disappeared in the MCLCE sample, which indicated a sufficient click reaction between alkynes and azides and the successful formation of the elastomer.
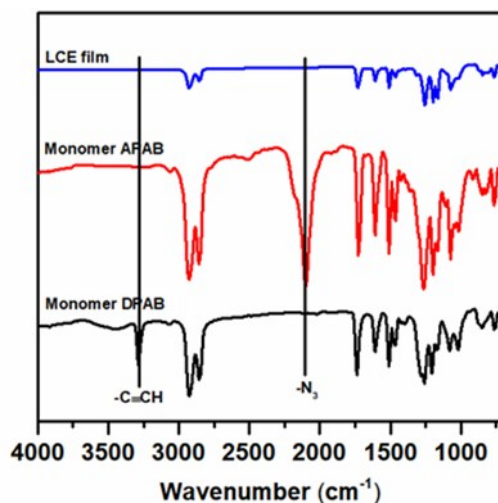
Fig. S5 FT-IR spectra of monomers DPDB, APAB and the corresponding MCLCE sample.

In order to understand the degree of crosslinking of the polydomain MCLCE, we measured the degree of crosslinking of the polydomain MCLCE measured by using a variable-temperature nuclear magnetic resonance analysis system (VTMR20-010V-T, Shanghai Niumag Electronic Technology Co., Ltd.), and the detailed data is included in **Table S1.** The crosslinking density of the MCLCE sample is calculated as ca. 25.01 × 10^{-4} mol/mL after crosslinked at 55 °C for 2 h.

Table S1 The crosslinking density data of the polydomain MCLCE sample.

Fitting model	M(t) = A*Exp(-t/T2-0.5*qMrl*t*t) + B*Exp(-t/T2) + C*Exp(-t/T2sol) + A0		
Fit initial value	A=0.60 B=0.40 C=0.01 T2=2.00 qMrl=3.00		

Sample: LCE	Temperature (°C): 90	NECH: 800	
Sequence: CPMG	**DRG1:** 3	**NS:** 64	
TW (ms): 1500	**DL1 (ms):** 0.02152	**DR:** 1	
SW (KHz): 200	**Sample density (g/mL):** 1	**RG1:** 20	

Sample name	T2 (ms)	T2sol (ms)	qMrl
LCE-1	0.49	4.3	293.71
LCE-2	0.52	4.52	279.26
LCE-3	0.49	4.55	298.09
Average	0.5	4.4567	290.3533
Standard deviation	1.73%	13.65%	985.36%
Relative standard deviation	3.46%	3.06%	3.39%

Sample name	A （Crosslinking proportion）	B （Proportion of catenary chain）	C （Proportion of free chain）
LCE-1	70.42	22.86	6.71
LCE-2	70.06	23.24	6.71
LCE-3	69.42	23.78	6.8
Average	69.9667%	23.2933%	6.74
Standard deviation	50.65%	46.23%	5.20%
Relative standard deviation	0.72%	1.98%	0.77%

Sample name	Density （g/ml）	Crosslinking density （*E-04 mol/mL）	Mc(kg/mol)
LCE-1	1.00	25.16	0.4
LCE-2	1.00	24.54	0.41
LCE-3	1.00	25.35	0.4
Average	1.00	25.0167	0.4033
Standard deviation	0.00%	42.36%	0.58%
Relative standard deviation	0.00%	1.69%	1.44%
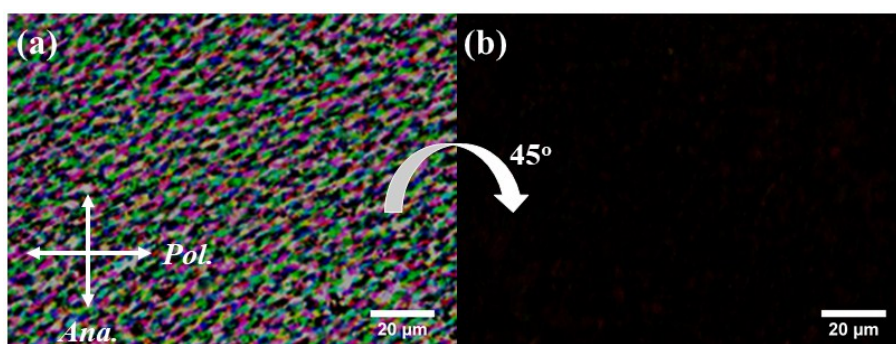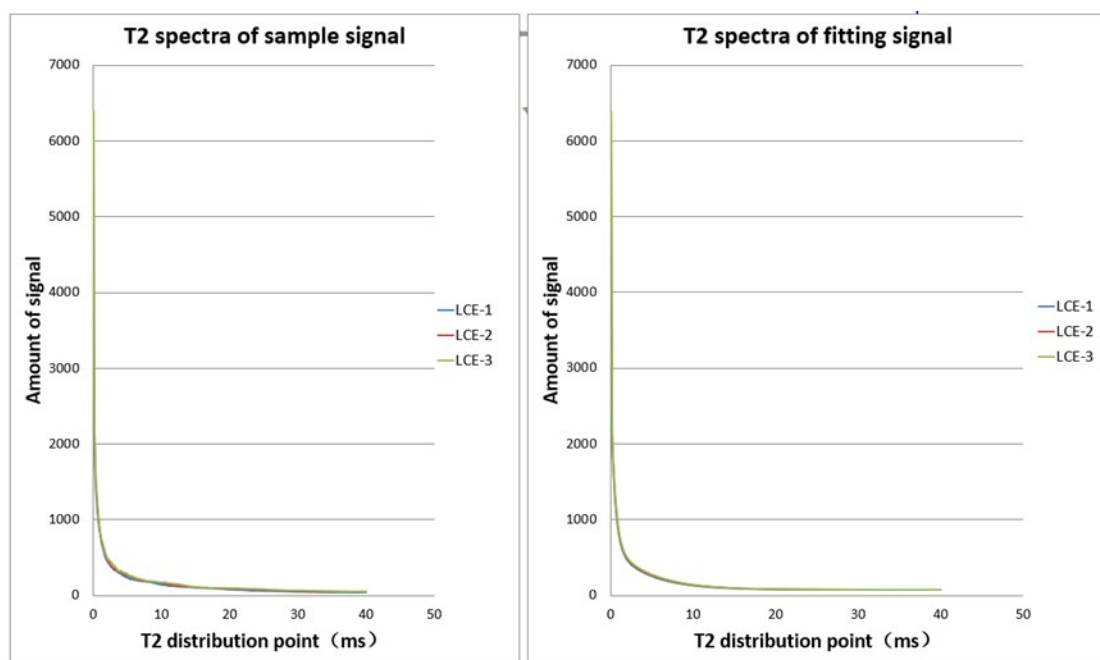
Fig. S6 POM images of uniaxially oriented LCE film.

As shown in **Figure S6**, the monodomain MCLCE exhibited a bright birefringent texture when its orientation was at an angle of 45° with the orthogonal polarizer/analyzer. When MCLCE film was rotated by ca. 45°, the transmittance of the film was the lowest at this time. This experiment proved the good quality of the mesogenic alignment of the MCLCE film.

To further confirm the T_g of monodomain MCLCE film, we utilized DMA to measure the storage modulus of the MCLCE film in the range of -25 to 140 °C. As shown in **Figure S7**, the glass transition (T_g) and LC-to-isotropic (T_{iso}) phase transition of LCE film were 23.9 °C and 106.9 °C, respectively.
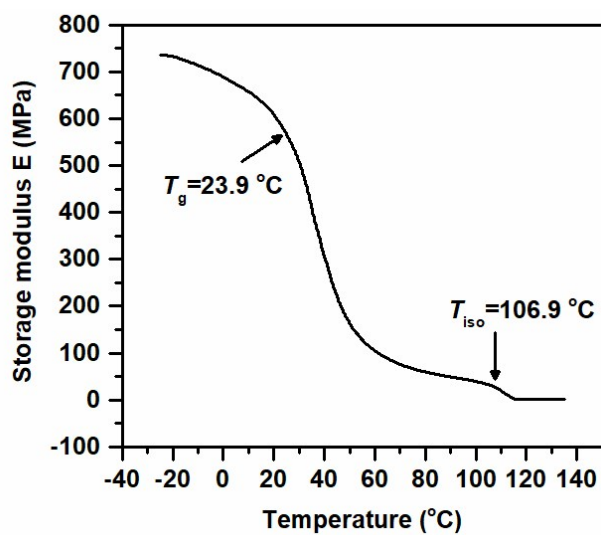
Fig. S7 Storage modulus of MCLCE sample measured as a function of temperature.
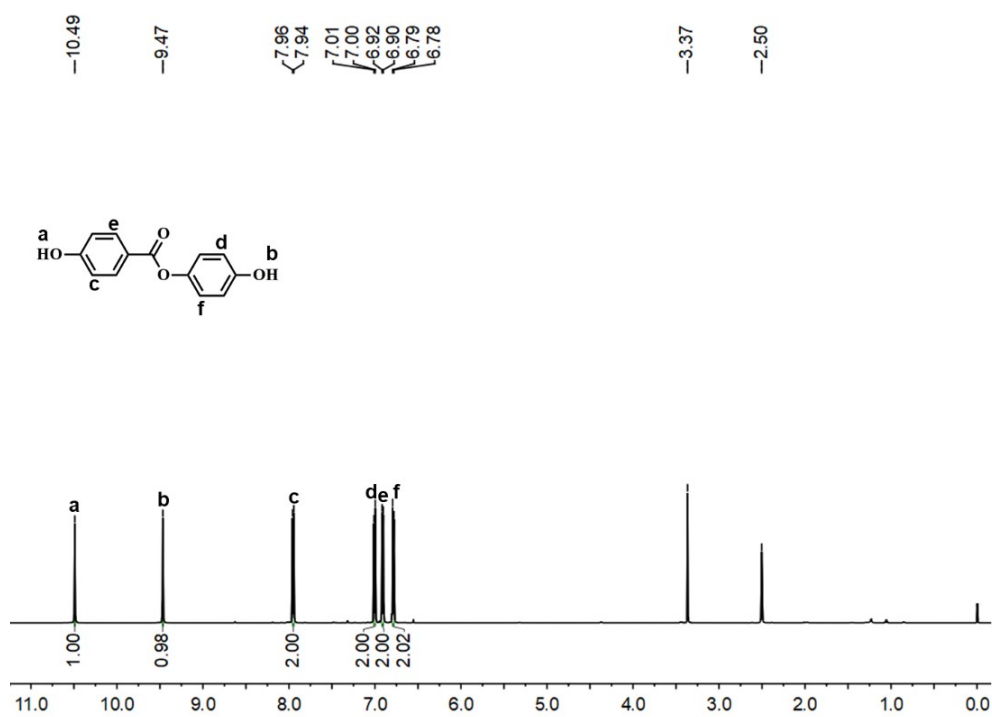
Fig. S8 ^{1}H NMR spectrum of compound **3**.
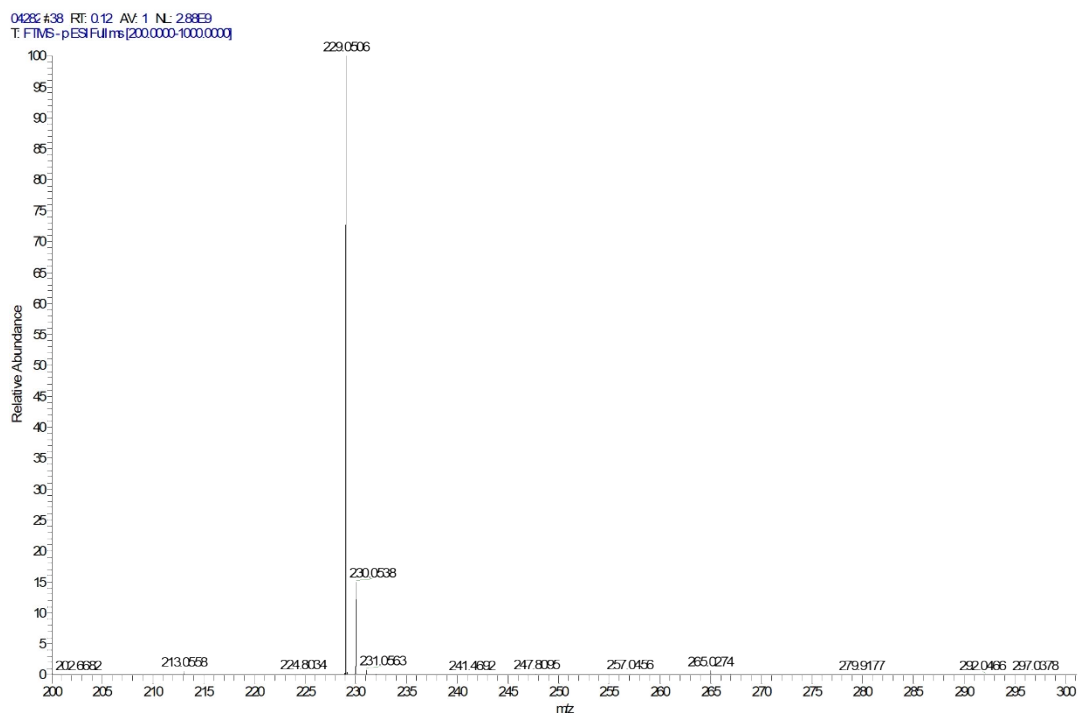
Fig. S9 ESI-MS spectrum of compound **3**.
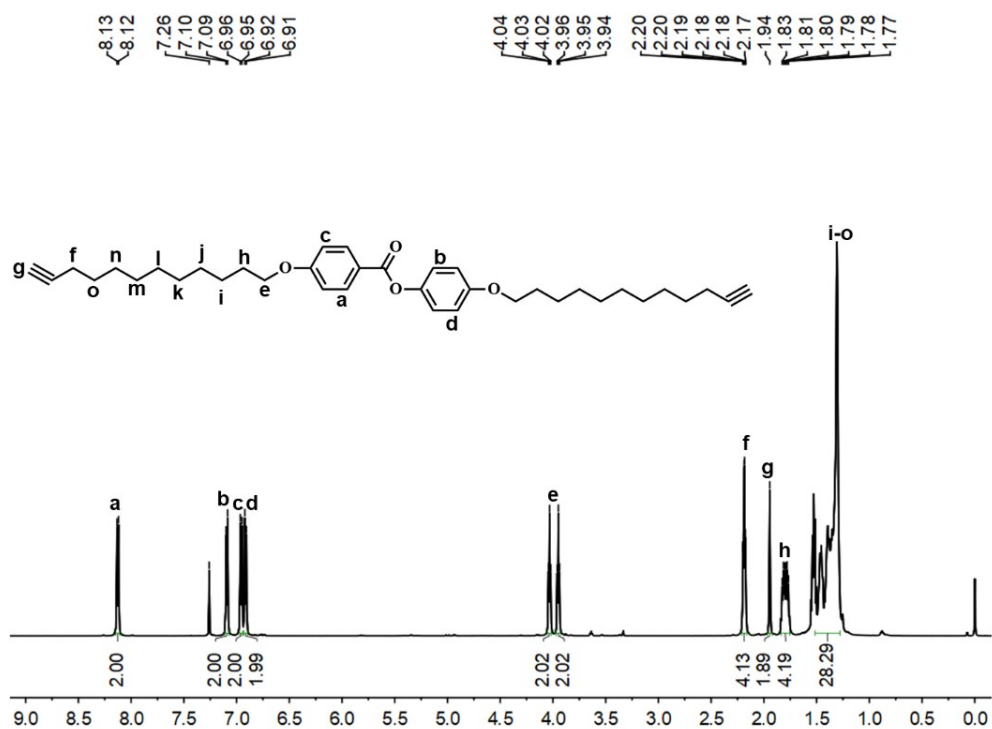
Fig. S10 ^{1}H NMR spectrum of DPDB.
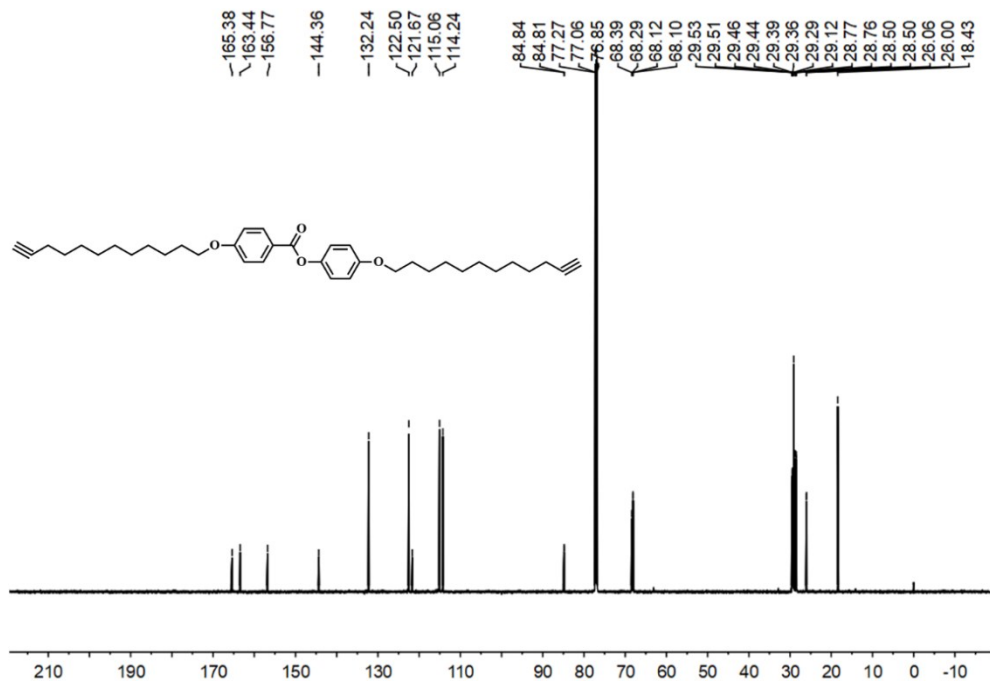
Fig. S11 ^{13}C NMR spectrum of DPDB.
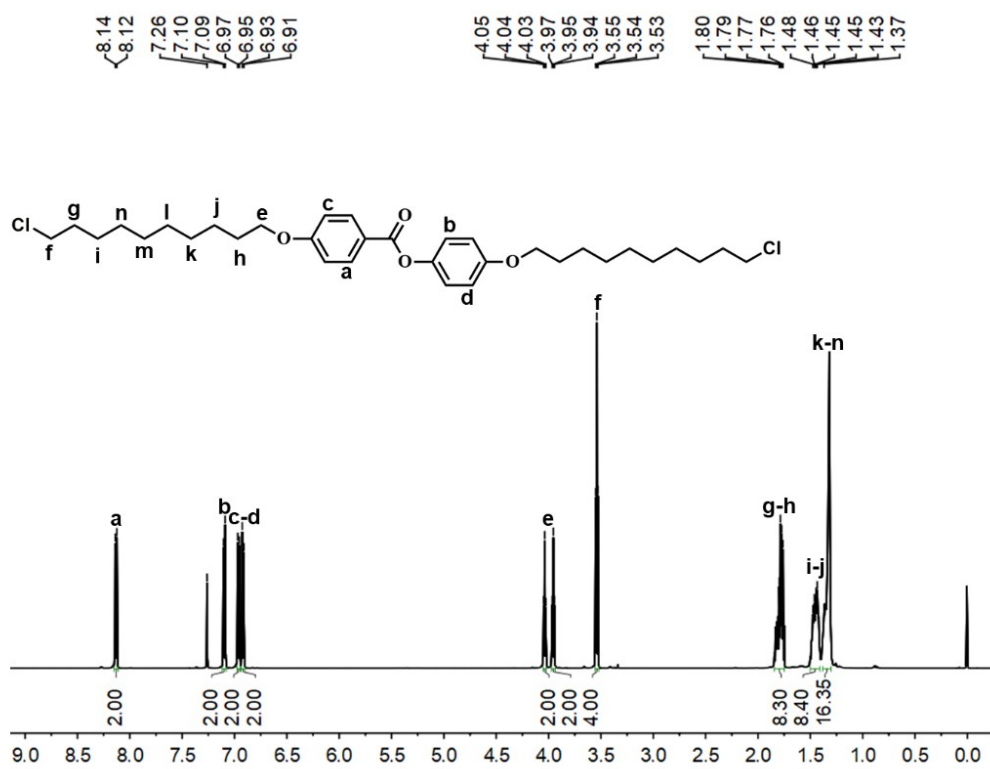
Fig. S12 ^{1}H NMR spectrum of compound **7**.
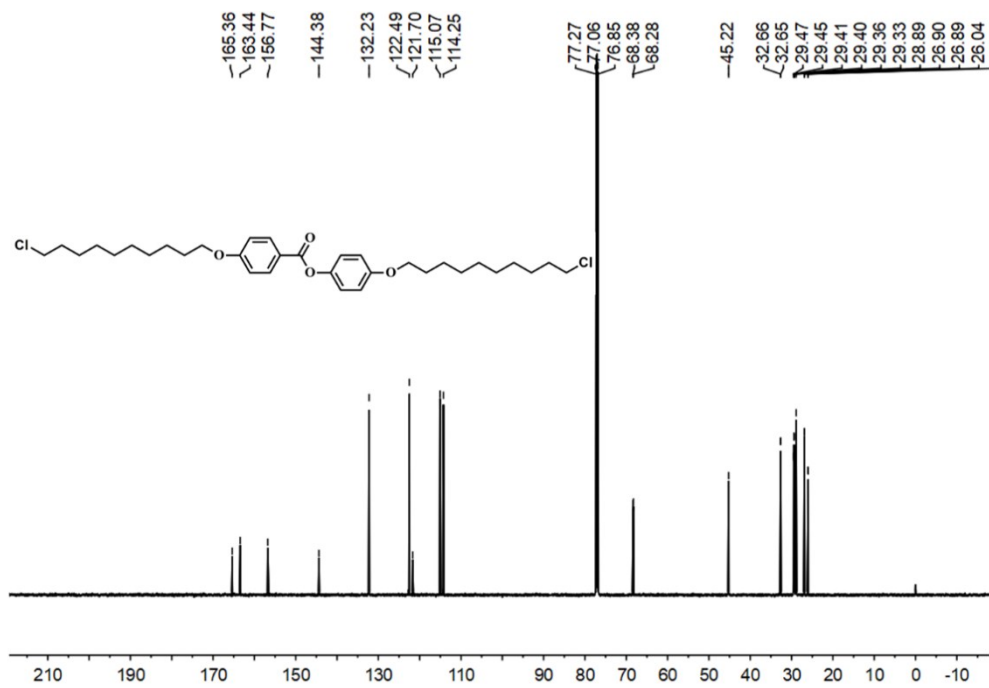
Fig. S13 ^{13}C NMR spectrum of compound **7**.
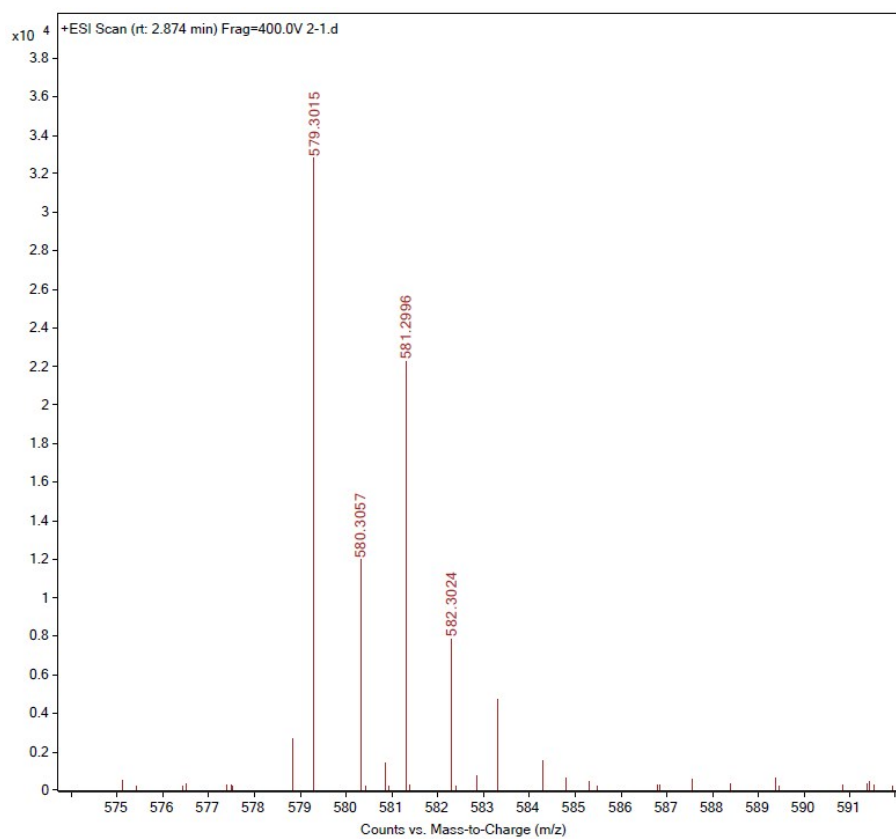
Fig. S14 ESI-MS spectrum of compound **7**.
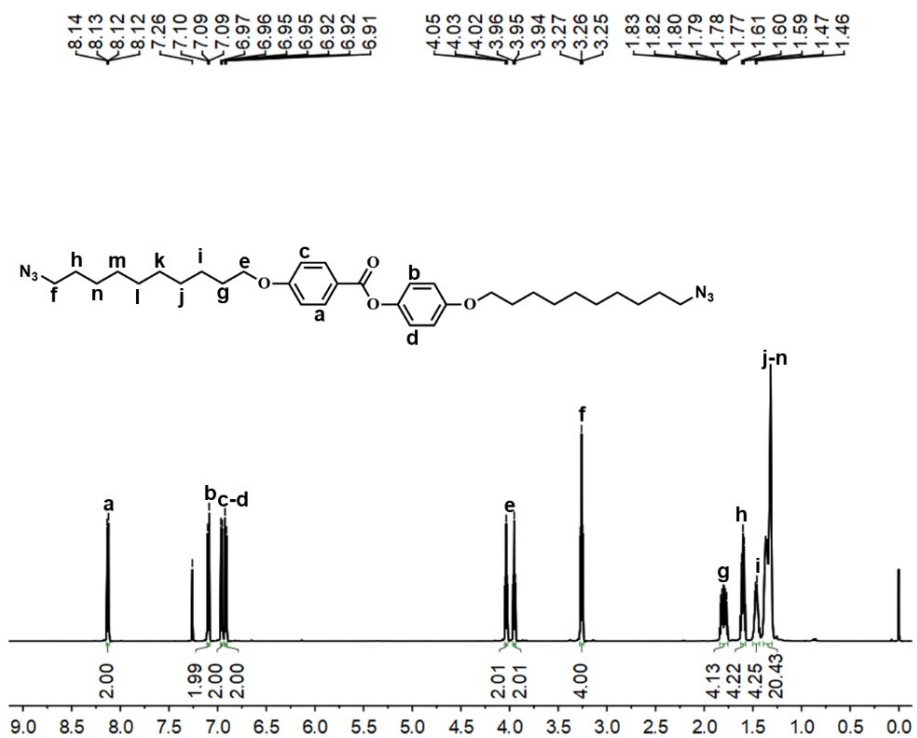
Fig. S15 ^{1}H NMR spectrum of APAB.
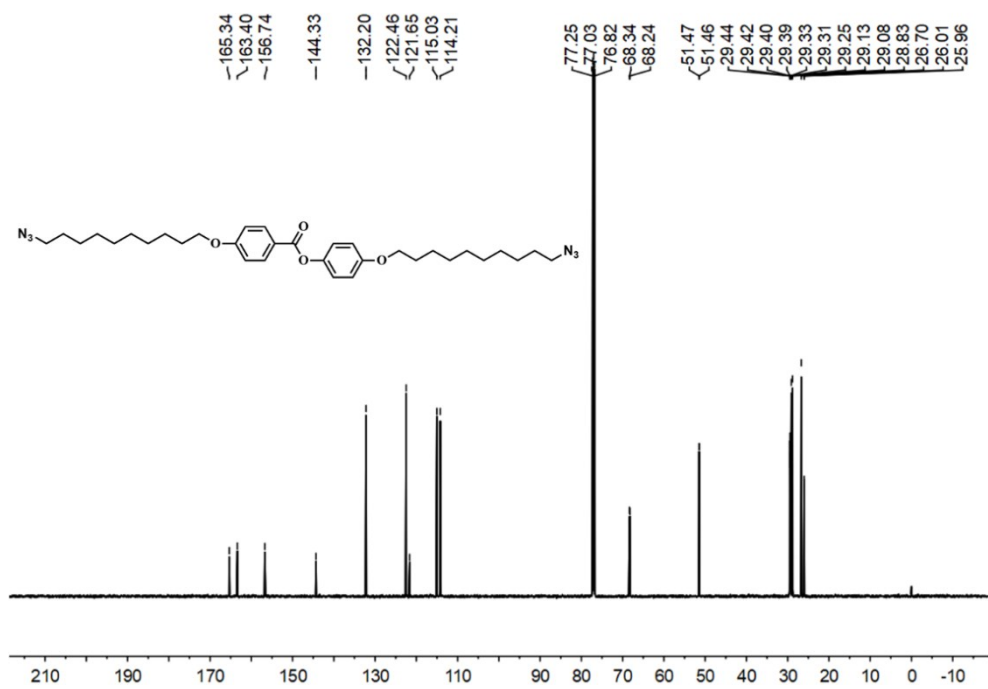
Fig. S16 ^{13}C NMR spectrum of APAB.
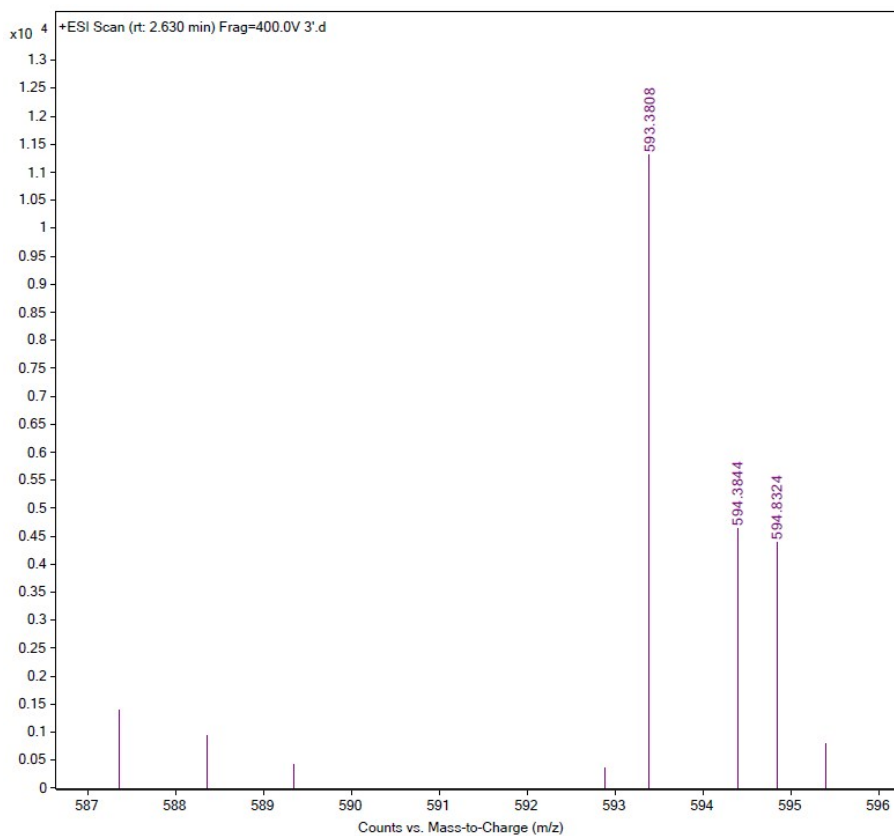
Fig. S17 ESI-MS spectrum of APAB.
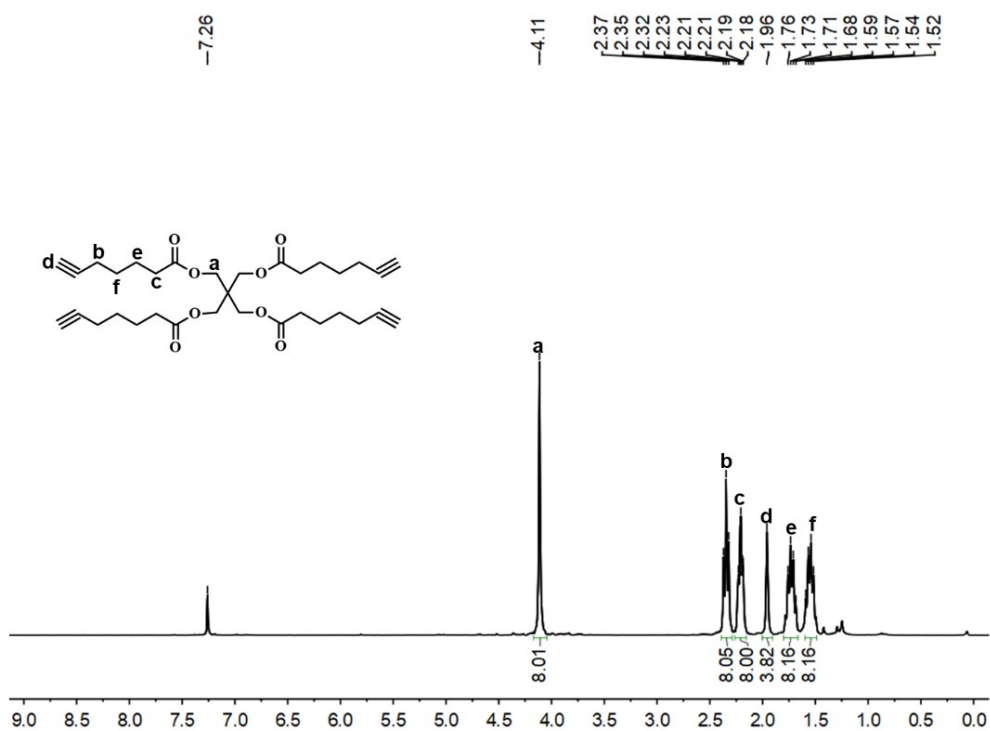
Fig. S18 ^{1}H NMR spectrum of crosslinker PTH.